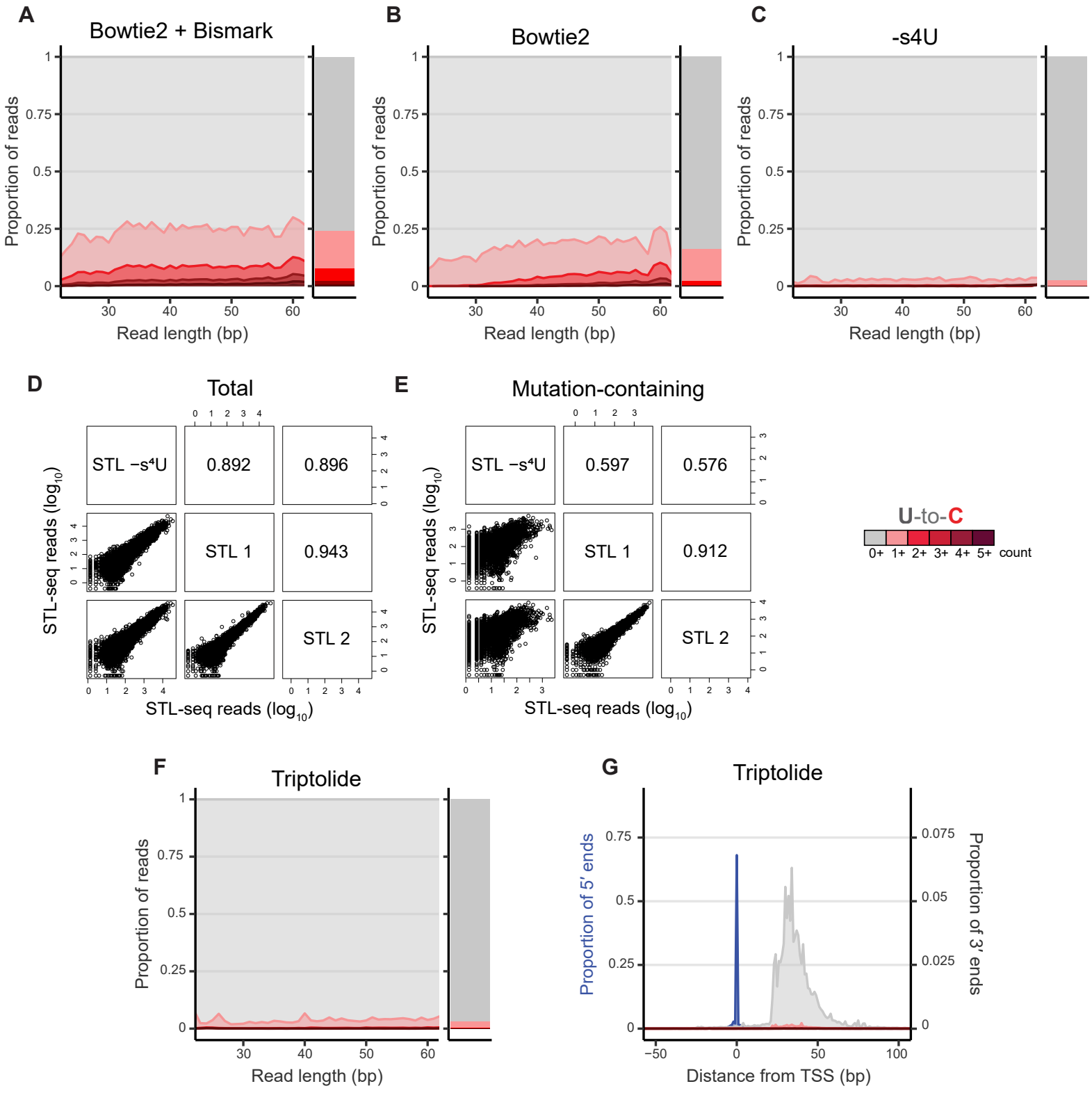
A
Bowtie2 + Bismark
B
Bowtie2
C
-s4U
Proportion of reads
Read length (bp)
D
Total
E
Mutation-containing
STL −s⁴U
STL 1
STL 2
0.892
0.896
0.943
0.597
0.576
0.912
STL-seq reads (log10)
U-to-C
0+ 1+ 2+ 3+ 4+ 5+ count
F
Triptolide
G
Triptolide
Proportion of 5′ ends
Proportion of 3′ ends
Distance from TSS (bp)

Figure S1.

Figure S1. STL-seq captures mutation information of newly synthesized short, capped transcripts, Related to Figure 1

(A, B, & C) The proportion of reads with varying numbers of mutations at each length. Reads are considered by absolute length, and each mutation level includes reads with the same or greater number of mutations. Reads were aligned with Bowtie2 combined with Bismark (A & C) or Bowtie2 alone (B) and either labeled (A & B) or unlabeled (C) with s^4U. The total proportion of reads is colored by number of mutations and shown on the right.

(D) Pairs plots of total TSS read counts from STL-seq unlabeled and labeled samples. Read counts are plotted on the $\log_{10}$ scale and the Pearson correlation coefficient of each comparison is shown.

(E) Pairs plots of mutation-containing TSS read counts from STL-seq unlabeled and labeled samples. Read counts are plotted on the $\log_{10}$ scale and the Pearson correlation coefficient of each comparison is shown.

(F) Same as A-C but labeled under triptolide inhibition and aligned with Bismark.

(G) Metaplot of STL-seq read ends relative to the TSS location under triptolide inhibition. The single nucleotide location of the TSS (blue, 5′ end of read) and pausing position (grey and red, 3′ end of read) are depicted separately. The 3′ ends are colored by the read's mutational content while the 5′ ends are not. Read ends at each distance from the TSS for the labeled samples are shown as a proportion of the total number of reads. The proportion of 5′ ends corresponds to the left y-axis scale and the proportion of 3′ ends corresponds to the right y-axis scale.

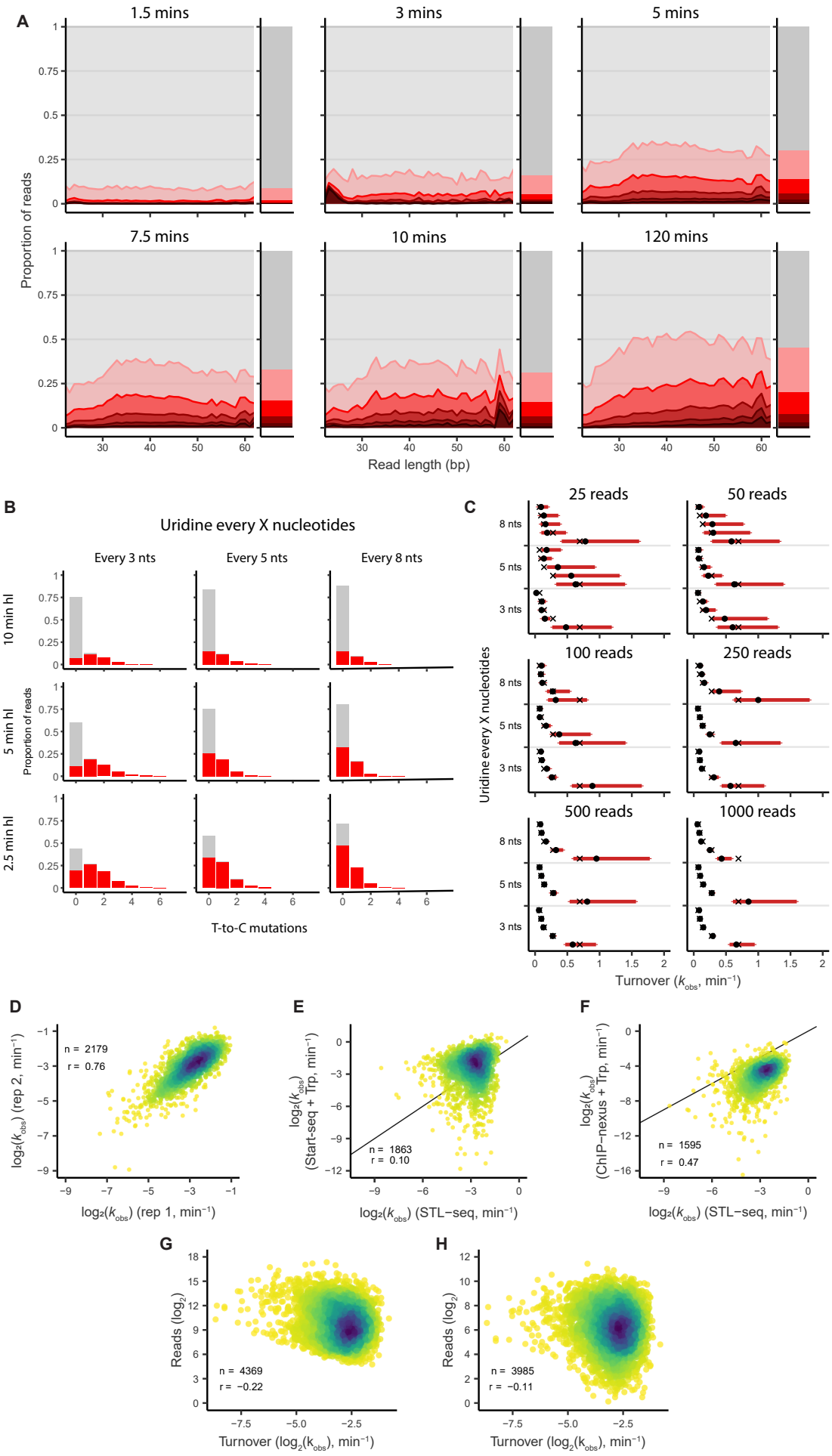
A
1.5 mins
3 mins
5 mins
7.5 mins
10 mins
120 mins
Proportion of reads
Read length (bp)
B
Uridine every X nucleotides
Every 3 nts
Every 5 nts
Every 8 nts
10 min hl
5 min hl
2.5 min hl
Proportion of reads
T-to-C mutations
C
25 reads
50 reads
100 reads
250 reads
500 reads
1000 reads
8 nts
5 nts
3 nts
Uridine every X nucleotides
Turnover (k_{obs}, min^{-1})
D
n = 2179
r = 0.76
log2(k_{obs}) (rep 2, min^{-1})
log2(k_{obs}) (rep 1, min^{-1})
E
n = 1863
r = 0.10
log2(k_{obs}) (Start-seq + Trp, min^{-1})
log2(k_{obs}) (STL−seq, min^{-1})
F
n = 1595
r = 0.47
log2(k_{obs}) (ChIP−nexus + Trp, min^{-1})
log2(k_{obs}) (STL−seq, min^{-1})
G
n = 4369
r = −0.22
Reads (log2)
Turnover (log2(k_{obs}), min^{-1})
H
n = 3985
r = −0.11
Reads (log2)
Turnover (log2(k_{obs}), min^{-1})

Figure S2.

Figure S2. Binomial modeling of STL-seq mutation data, Related to Figure 2

(A) The proportion of reads with varying numbers of mutations at each length when labeled for varying times with s^4U. Reads are considered by absolute length and each mutation level includes reads with the same or greater number of mutations. The total proportion of reads is colored by number of mutations and shown on the right of the plot for each label time.

(B) Simulated STL-seq mutational content of TSSs with various pausing half-lives (hl) and uridine content. Reads are colored by whether they are considered new (red) and synthesized during the label time or old (grey) and synthesized prior to labeling. See STAR methods for details of simulated data.

(C) Using the model to estimate the rate constant of simulated data generated as in B in addition to varying degrees of coverage. The true rate constant is indicated with a cross. The median value of the posterior estimate is indicated with a solid circle and the 80% credible interval is indicated by red bars. See STAR methods for details of simulated data.

(D) Correlation plot comparing estimates from single STL-seq replicates. Plotted points represent the median value of the posterior estimate. The density of plotted points is indicated by color (blue, high; yellow, low). The Pearson correlation coefficient is shown.

(E) Correlation plot comparing $\hat{k}_{obs}$ estimates made with STL-seq and previously published Start-seq data under Trp inhibition. The median value of the STL-seq posterior estimate is plotted and the 1:1 line is shown. The density of plotted points is indicated by color (blue, high; yellow, low). The Pearson correlation coefficient is shown.

(F) Correlation plot comparing $\hat{k}_{obs}$ estimates made with STL-seq and previously published ChIP-nexus data under Trp inhibition. The median value of the STL-seq posterior estimate is plotted and the 1:1 line is shown. The density of plotted points is indicated by color (blue, high; yellow, low). The Pearson correlation coefficient is shown.

(G) Correlation plot comparing STL-seq $\hat{k}_{obs}$ estimates and STL-seq read counts at each TSS. The median value of the STL-seq posterior estimate is plotted. The density of plotted points is indicated by color (blue, high; yellow, low). The Pearson correlation coefficient is shown.

(H) As in G but comparing STL-seq $\hat{k}_{obs}$ estimates and PRO-seq read counts in the promoter-proximal region of each TSS.

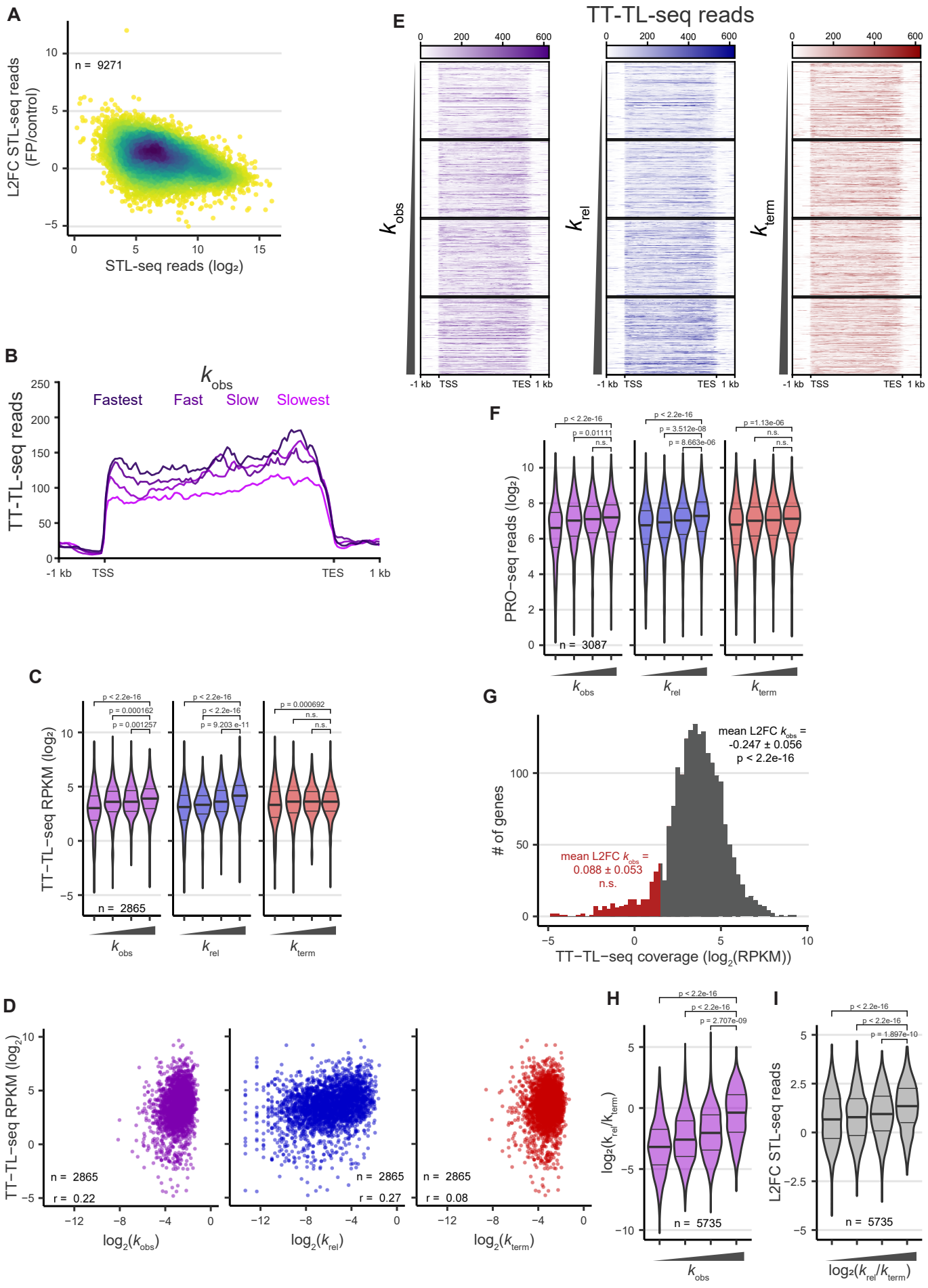
A
L2FC STL-seq reads (FP/control)
STL-seq reads (log₂)
n = 9271
B
TT-TL-seq reads
k_{obs}
Fastest
Fast
Slow
Slowest
-1 kb
TSS
TES
1 kb
C
TT−TL−seq RPKM (log₂)
p < 2.2e-16
p = 0.000162
p = 0.001257
p < 2.2e-16
p = 9.203 e-11
p = 0.000692
n.s.
n = 2865
k_{obs}
k_{rel}
k_{term}
D
TT−TL−seq RPKM (log₂)
n = 2865
r = 0.22
r = 0.27
r = 0.08
$log_2(k_{obs})$
$log_2(k_{rel})$
$log_2(k_{term})$
E
TT-TL-seq reads
k_{obs}
k_{rel}
k_{term}
F
PRO−seq reads (log₂)
p < 2.2e-16
p = 0.01111
n.s.
p = 3.512e-08
p = 8.663e-06
p =1.13e-06
n = 3087
G
# of genes
mean L2FC k_{obs} = -0.247 ± 0.056
p < 2.2e-16
mean L2FC k_{obs} = 0.088 ± 0.053
n.s.
TT−TL−seq coverage (log_2(RPKM))
H
$log_2(k_{rel}/k_{term})$
p < 2.2e-16
p = 2.707e-09
n = 5735
I
L2FC STL-seq reads
p < 2.2e-16
p = 1.897e-10
n = 5735
$log_2(k_{rel}/k_{term})$

Figure S3.

Figure S3. Release from the pause site predicts downstream transcriptional activity, Related to Figure 3

(A) The change in normalized STL-seq reads at all TSS upon flavopiridol inhibition plotted versus the average normalized STL-seq read count in untreated controls. The density of plotted points is indicated by color (blue, high; yellow, low).

(B) Metaplots of TT-TL-seq signal grouped into even quartiles by total observed turnover of the respective TSS. Coverage is determined over 50 nt bins.

(C) The distribution of TT-TL-seq coverage over the entire gene body by RPKM. Genes are grouped into even quartiles by total observed turnover, release, or termination of the respective TSS. Significance was assessed by a two-sided Wilcoxon rank sum test.

(D) Correlation plot comparing $\hat{k}_{obs}$, $\hat{k}_{rel}$, or $\hat{k}_{term}$ estimates made with STL-seq and TT-TL-seq coverage in RPKM. The median value of the STL-seq posterior estimate is plotted. The Pearson correlation coefficient is shown.

(E) Heat maps of TT-TL-seq data grouped as in C and ordered by the indicated rate constant.

(F) The distribution of PRO-seq (Elrod et al., 2019) reads over the region from 0.5 kb to 1.5 kb downstream of the TSS. Genes are grouped into even quartiles by total observed turnover, release, or termination of the respective TSS. Significance was assessed by a two-sided Wilcoxon rank sum test.

(G) Histogram of RPKM values for genes in TT-TL-seq data. The red highlighted region represents the 10% of genes with the least coverage. The mean $\log_2$ fold change of $\hat{k}_{obs}$ upon FP treatment and standard error are shown for TSSs of the bottom 10% of genes (red) or the entire genome (black). Statistical difference from zero was assessed with a one-sample Wilcoxon signed rank test.

(H) The distribution of the $\log_2$ ratio of the release rate to termination rate at all TSSs grouped into even quartiles by the total observed turnover. Significance was assessed by a two-sided Wilcoxon rank sum test.

(I) The distribution of the $\log_2$ fold change in normalized STL-seq read counts upon flavopiridol inhibition at all TSSs grouped into even quartiles by the $\log_2$ ratio of the release rate to termination rate. Significance was assessed by a two-sided Wilcoxon rank sum test.

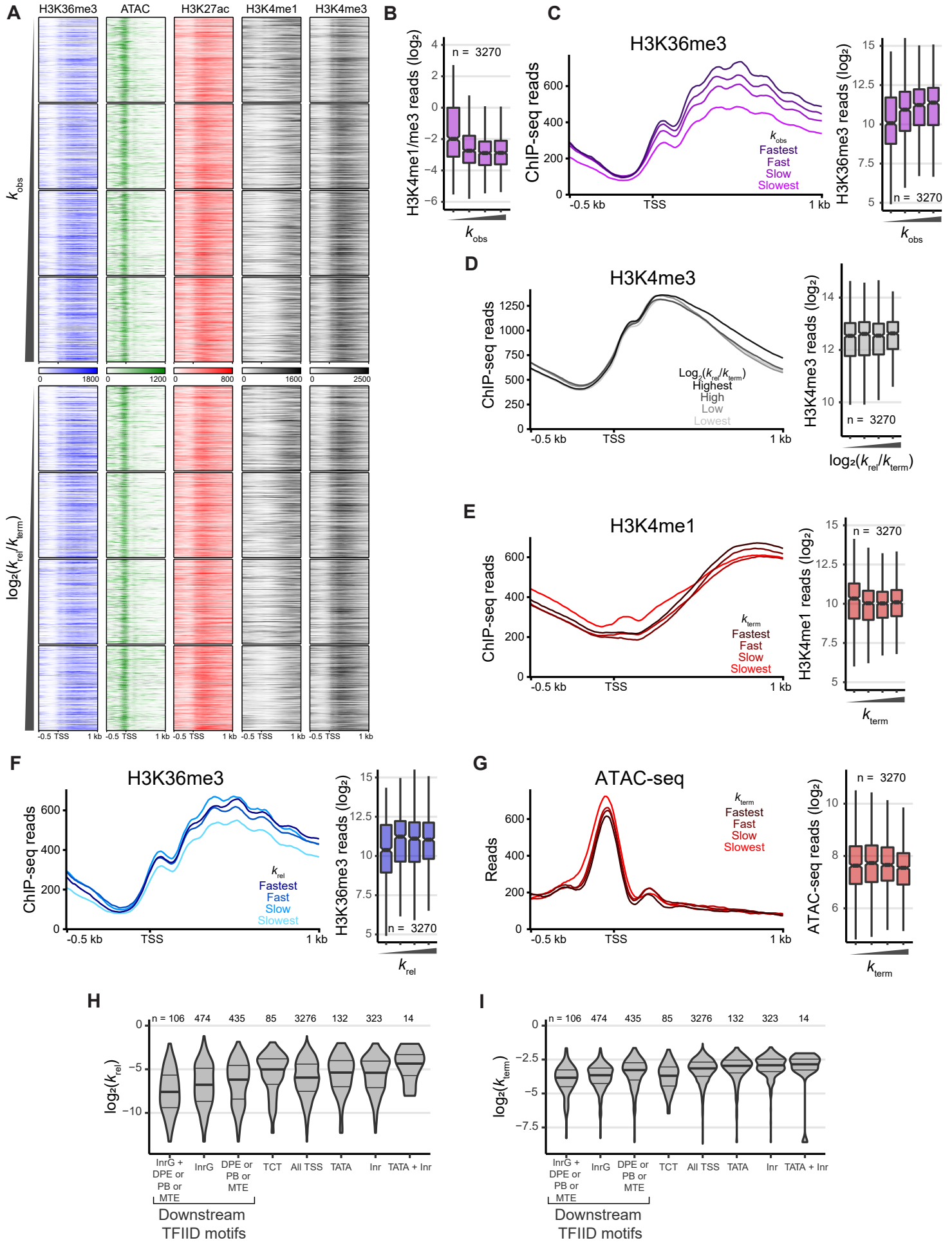
A
H3K36me3
ATAC
H3K27ac
H3K4me1
H3K4me3
k_{obs}
$\log_2(k_{rel}/k_{term})$
0 1800
0 1200
0 800
0 1600
0 2500
-0.5 TSS 1 kb
B
H3K4me1/me3 reads ($\log_2$)
n = 3270
k_{obs}
C
H3K36me3
ChIP-seq reads
k_{obs}
Fastest
Fast
Slow
Slowest
-0.5 kb
TSS
1 kb
H3K36me3 reads ($\log_2$)
n = 3270
D
H3K4me3
ChIP-seq reads
$\text{Log}_2(k_{rel}/k_{term})$
Highest
High
Low
Lowest
H3K4me3 reads ($\log_2$)
$\log_2(k_{rel}/k_{term})$
E
H3K4me1
ChIP-seq reads
k_{term}
H3K4me1 reads ($\log_2$)
F
H3K36me3
k_{rel}
G
ATAC-seq
Reads
ATAC-seq reads ($\log_2$)
H
$\log_2(k_{rel})$
n = 106 474 435 85 3276 132 323 14
InrG + DPE or PB or MTE
InrG
DPE or PB or MTE
TCT
All TSS
TATA
Inr
TATA + Inr
Downstream TFIID motifs
I
$\log_2(k_{term})$

Figure S4.

Figure S4. Chromatin structure defines unique profiles of pausing kinetics, Related to Figure 4

(A) Heat maps of ATAC-seq (Elrod et al., 2019) and ChIP-seq H3K27ac, H3K4me1, H3K4me3 (Henriques et al., 2018), and H3K36me3 (Chen et al., 2012) around promoters grouped into even quartiles and ordered by total turnover or $\log_2$ ratio of the release rate to the termination rate of the respective TSS. Heatmaps are centered on the STL-seq TSS with a window of 0.5 kb upstream and 1 kb downstream.

(B) The $\log_2$ ratio of H3K4me1 to H3K4me3 ChIP-seq reads in the window 0.5 kb upstream and 1 kb downstream of the promoter TSS, grouped into even quartiles by total turnover (n = 3270 promoters). Significance was assessed by a two-sided Wilcoxon rank sum test.

(C) Metaplot (left) and read count distribution (right) of H3K36me3 ChIP-seq data around promoters with a window of 0.5 kb upstream and 1 kb downstream of the TSS, grouped into even quartiles by total turnover.

(D) Metaplot (left) and read count distribution (right) of H3K4me3 ChIP-seq data around promoters with a window of 0.5 kb upstream and 1 kb downstream of the TSS, grouped into even quartiles by the $\log_2$ ratio of the release rate to the termination rate.

(E) Metaplot (left) and read count distribution (right) of H3K4me1 ChIP-seq data around promoters with a window of 0.5 kb upstream and 1 kb downstream of the TSS, grouped into even quartiles by termination.

(F) Same as C but grouped into even quartiles by pause release.

(G) Metaplot (left) and read count distribution (right) of ATAC-seq data around promoters with a window of 0.5 kb upstream and 1 kb downstream of the TSS grouped into even quartiles by termination.

(H and I) The distribution of the release rate (H) or termination rate constants (I) at promoters grouped by motif content. The pause button (PB), downstream promoter element (DPE), and motif ten element (MTE) were grouped together such that promoters may have one or a combination of these in the downstream region.

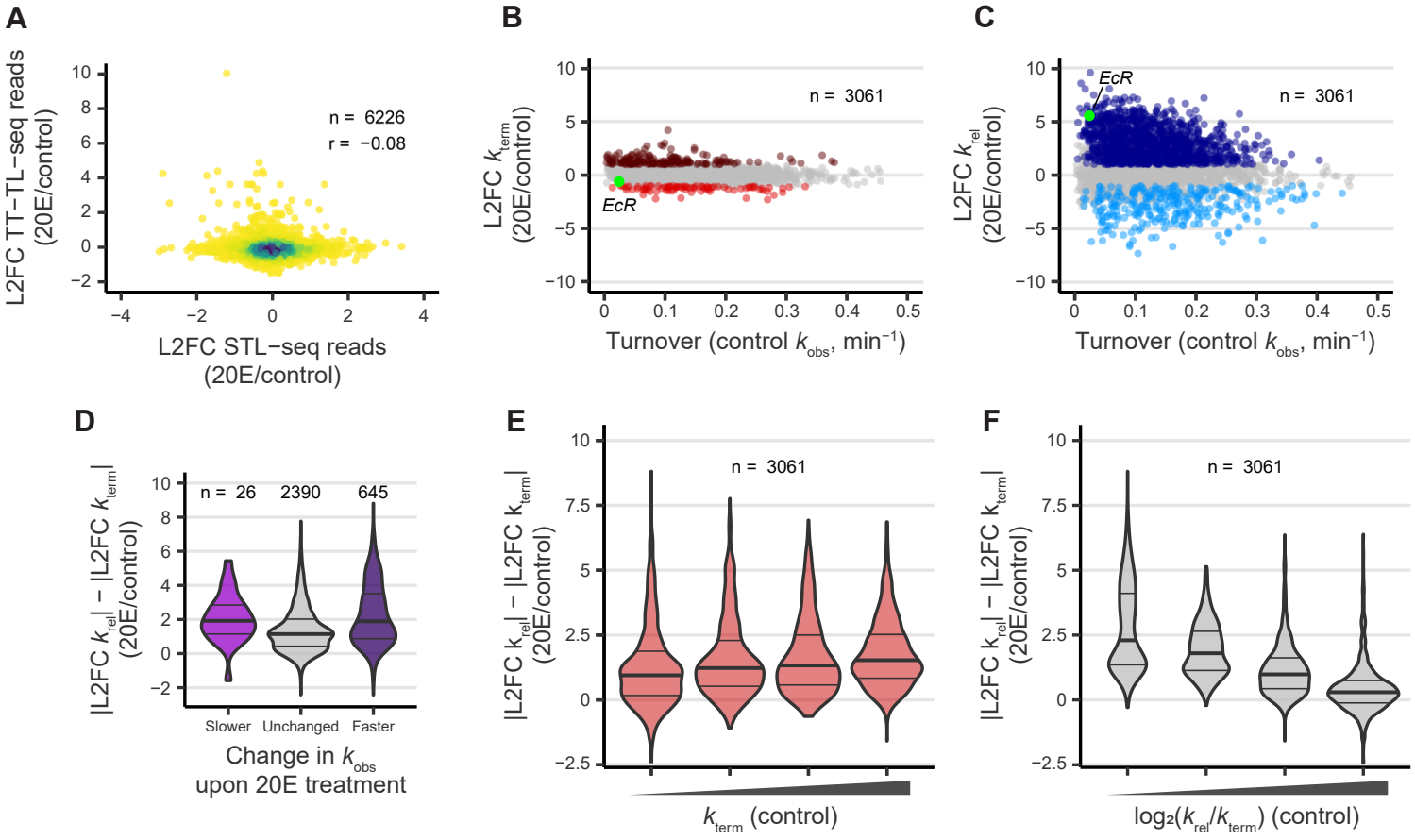
A
L2FC TT−TL−seq reads (20E/control)
L2FC STL−seq reads (20E/control)
n = 6226
r = −0.08
B
L2FC k_{term} (20E/control)
Turnover (control k_{obs}, min^{-1})
n = 3061
EcR
C
L2FC k_{rel} (20E/control)
Turnover (control k_{obs}, min^{-1})
n = 3061
EcR
D
|L2FC k_{rel}| − |L2FC k_{term}| (20E/control)
n = 26
2390
645
Slower
Unchanged
Faster
Change in k_{obs} upon 20E treatment
E
|L2FC k_{rel}| − |L2FC k_{term}| (20E/control)
n = 3061
k_{term} (control)
F
|L2FC k_{rel}| − |L2FC k_{term}| (20E/control)
n = 3061
$\log_2(k_{rel}/k_{term})$ (control)

Figure S5.

Figure S5. Termination is rarely regulated in response to hormone stimulus, Related to Figure 5

(A) The $\log_2$ fold change in normalized STL-seq reads at all TSS upon 20E treatment versus the $\log_2$ fold change in normalized TT-TL-seq read counts of the associated gene upon hormonal treatment. The density of plotted points is indicated by color (blue, high; yellow, low). The Pearson correlation coefficient is shown.

(B and C) The total observed turnover rate constants plotted versus the $\log_2$ fold change in termination (B) or release (C) upon 20E stimulus. Points are colored if the 80% credible interval of the $\log_2$ fold change does not overlap zero and the median value is greater than 1 (dark red/blue) or less than -1 (light red/blue).

(D) The difference between the magnitudes of the $\log_2$ fold change of release and termination grouped by the change in the total turnover as determined in Figure 6B.

(E) The difference between the magnitudes of the $\log_2$ fold change of release and termination grouped by the change into even quartiles by termination.

(F) The difference between the magnitudes of the $\log_2$ fold change of release and termination grouped by the change into even quartiles by the $\log_2$ ratio of the release rate to the termination rate.

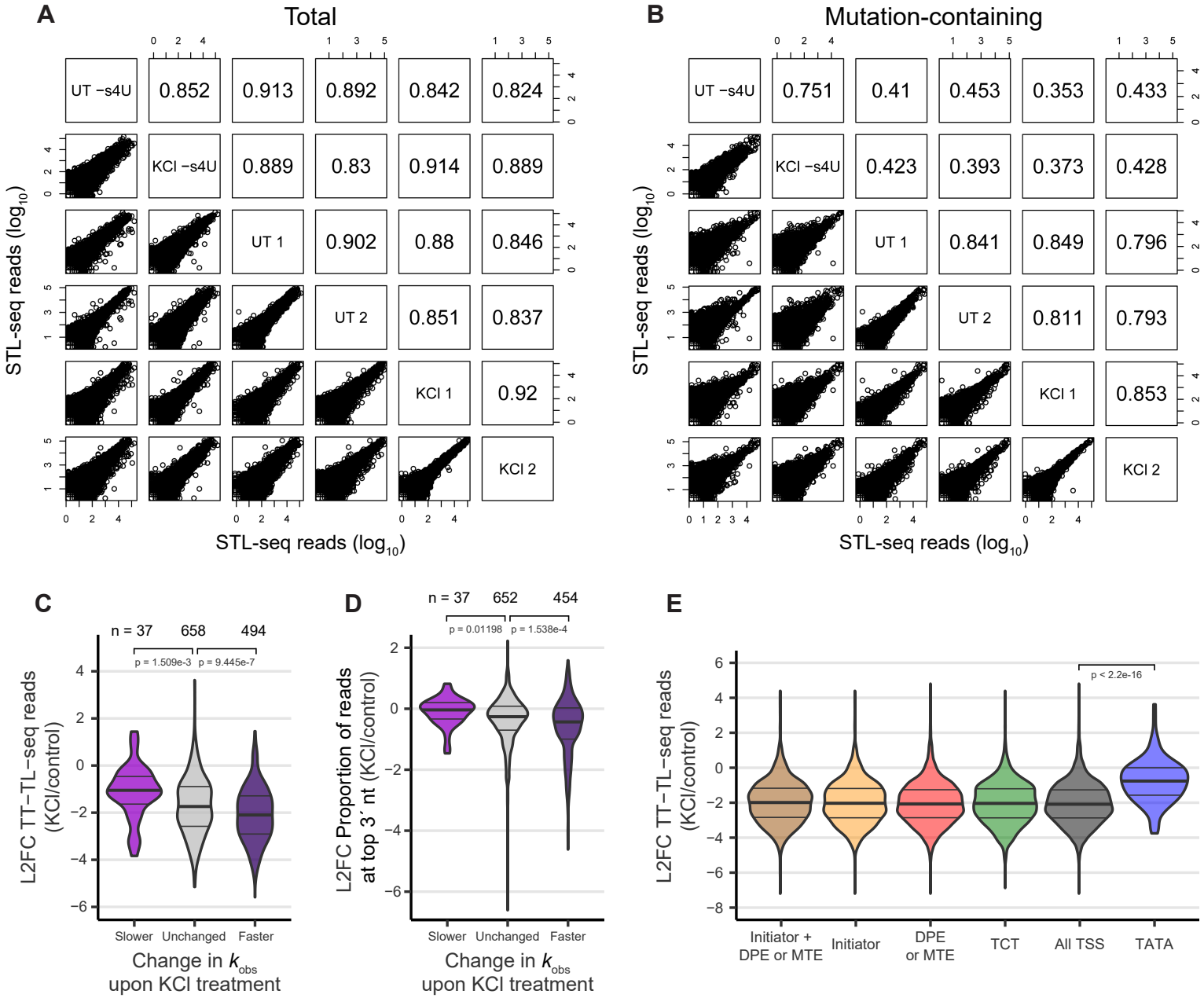
A
Total
UT −s4U
KCl −s4U
UT 1
UT 2
KCl 1
KCl 2
0.852
0.913
0.892
0.842
0.824
0.889
0.83
0.914
0.889
0.902
0.88
0.846
0.851
0.837
0.92
STL-seq reads (log10)
B
Mutation-containing
0.751
0.41
0.453
0.353
0.433
0.423
0.393
0.373
0.428
0.841
0.849
0.796
0.811
0.793
0.853
C
n = 37 658 494
p = 1.509e-3 p = 9.445e-7
L2FC TT−TL−seq reads (KCl/control)
Slower Unchanged Faster
Change in kobs upon KCl treatment
D
n = 37 652 454
p = 0.01198 p = 1.538e-4
L2FC Proportion of reads at top 3′ nt (KCl/control)
E
p < 2.2e-16
Initiator + DPE or MTE
Initiator
DPE or MTE
TCT
All TSS
TATA

Figure S6.

Figure S6. Increased termination at the pause site causes widespread transcriptional repression upon hyperosmotic stress in human cells, Related to Figure 6

(A) Pairs plots of total TSS read counts from STL-seq unlabeled and labeled samples under normal and hyperosmotic stress conditions. Read counts are plotted on the $\log_{10}$ scale and the Pearson correlation coefficient of each comparison is shown.

(B) Pairs plots of mutation-containing TSS read counts from STL-seq unlabeled and labeled samples under normal and hyperosmotic stress conditions. Read counts are plotted on the $\log_{10}$ scale and the Pearson correlation coefficient of each comparison is shown.

(C) Distribution of the $\log_2$ fold change of TT-TL-seq signal upon hyperosmotic stress grouped by the change in turnover of the TSS called to each gene. Significance was assessed by a two-sided Wilcoxon rank sum test.

(D) Distribution of the $\log_2$ fold change of the proportion of reads with 3′ ends located at the most frequent pause position grouped by the change in turnover of the scRNA. At each promoter, the most common position of the 3′ read end is identified, and all reads are considered by their 3′ end relative to the most common. The change in the proportion of reads at the most common position upon hyperosmotic stress is plotted.

(E) Distribution of the $\log_2$ fold change of TT-TL-seq signal upon hyperosmotic stress grouped by the motif content of the associated STL-seq TSS. Significance was assessed by a two-sided Wilcoxon rank sum test.

Table S1. STL-seq oligos used in this study. Related to STAR methods.

Name	Oligo
STL-seq custom 3´ DNA adapter	rAppGATCGGAAGAGCACACGTCTG /3'SPACER C3/
STL-seq custom 5´ RNA adapter	rUrArCrArCrGrArCrGrCrUrCrUrUrCrCrGrArUrCrUrCrGrArUrC
STL-seq custom RT primer	CAGACGTGTGCTCTTCC
STL-seq custom 5' indexing primer 1	AATGATACGGCGACCACCGAGATCTACACTATAGCCTACACT CTTTCCCTACACGACGCTCTTCCGATCT
STL-seq custom 5' indexing primer 2	AATGATACGGCGACCACCGAGATCTACACATAGAGGCACAC TCTTTCCCTACACGACGCTCTTCCGATCT
STL-seq custom 5' indexing primer 3	AATGATACGGCGACCACCGAGATCTACACCCTATCCTACACT CTTTCCCTACACGACGCTCTTCCGATCT
STL-seq custom 5' indexing primer 4	AATGATACGGCGACCACCGAGATCTACACGGCTCTGAACAC TCTTTCCCTACACGACGCTCTTCCGATCT
STL-seq custom 5' indexing primer 5	AATGATACGGCGACCACCGAGATCTACACAGGCGAAGACAC TCTTTCCCTACACGACGCTCTTCCGATCT
STL-seq custom 5' indexing primer 6	AATGATACGGCGACCACCGAGATCTACACTAATCTTAACACT CTTTCCCTACACGACGCTCTTCCGATCT
STL-seq custom 5' indexing primer 7	AATGATACGGCGACCACCGAGATCTACACCAGGACGTACAC TCTTTCCCTACACGACGCTCTTCCGATCT
STL-seq custom 5' indexing primer 8	AATGATACGGCGACCACCGAGATCTACACGTACTGACACAC TCTTTCCCTACACGACGCTCTTCCGATCT
STL-seq custom 3' indexing primer 1	CAAGCAGAAGACGGCATACGAGATCGAGTAATGTGACTGGA GTTCAGACGTGTGCTCTTCCGATC
STL-seq custom 3' indexing primer 2	CAAGCAGAAGACGGCATACGAGATCTCCGGAGTGACTGGAG TTCAGACGTGTGCTCTTCCGATC
STL-seq custom 3' indexing primer 3	CAAGCAGAAGACGGCATACGAGATAATGAGCGGTGACTGGA GTTCAGACGTGTGCTCTTCCGATC
STL-seq custom 3' indexing primer 4	CAAGCAGAAGACGGCATACGAGATGGAATCTCGTGACTGGA GTTCAGACGTGTGCTCTTCCGATC
STL-seq custom 3' indexing primer 5	CAAGCAGAAGACGGCATACGAGATTTCTGAATGTGACTGGA GTTCAGACGTGTGCTCTTCCGATC
STL-seq custom 3' indexing primer 6	CAAGCAGAAGACGGCATACGAGATACGAATTCGTGACTGGA GTTCAGACGTGTGCTCTTCCGATC
STL-seq custom 3' indexing primer 7	CAAGCAGAAGACGGCATACGAGATAGCTTCAGGTGACTGGA GTTCAGACGTGTGCTCTTCCGATC
STL-seq custom 3' indexing primer 8	CAAGCAGAAGACGGCATACGAGATGCGCATTAGTGACTGGA GTTCAGACGTGTGCTCTTCCGATC